SCIENTIFIC REPORTS

OPEN

SUBJECT AREAS:
VASCULAR DISEASES
ATHEROSCLEROSIS

Received
31 March 2014

Accepted
13 June 2014

Published
1 July 2014

Correspondence and requests for materials should be addressed to B.X.Z. (bxzhao@sdu.edu.cn) or J.Y.M. (miaojy@sdu.edu.cn)

* These authors contributed equally to this work.

An activator of mTOR inhibits oxLDL-induced autophagy and apoptosis in vascular endothelial cells and restricts atherosclerosis in apolipoprotein $E^{-/-}$ mice

Nan Peng[1]*, Ning Meng[2,3]*, ShengQing Wang[3], Fei Zhao[1], Jing Zhao[1], Le Su[1], ShangLi Zhang[1], Yun Zhang[4], BaoXiang Zhao[3] & JunYing Miao[1,4]

[1]Shandong Provincial Key Laboratory of Animal Cells and Developmental Biology, School of Life Science, Shandong University, Jinan 250100, China, [2]School of Biological Science and Technology, University of Jinan, Jinan 250022, China, [3]Institute of Organic Chemistry, School of Chemistry and Chemical Engineering, Shandong University, Jinan 250100, China, [4]The Key Laboratory of Cardiovascular Remodeling and Function Research, Chinese Ministry of Education and Chinese Ministry of Health, Shandong University Qilu Hospital, Jinan, 250012, China.

Oxidized low-density lipoprotein (oxLDL) inhibits mammalian target of rapamycin (mTOR) and induces autophagy and apoptosis in vascular endothelial cells (VECs) that play very critical roles for the cardiovascular homostasis. We recently defined 3-benzyl-5-((2-nitrophenoxy) methyl)-dihydrofuran-2(3H)-one (3BDO) as a new activator of mTOR. Therefore, we hypothesized that 3BDO had a protective role in VECs and thus stabilized atherosclerotic lesions in apolipoprotein $E^{-/-}$ ($apoE^{-/-}$) mice. Our results showed that oxLDL inhibited the activity of mTOR and increased the protein level of autophagy-related 13 (ATG13) and its dephosphorylation, thus inducing autophagy in human umbilical vein endothelial cells (HUVECs). All of these effects were strongly inhibited by 3BDO. *In vivo* experiments confirmed that 3BDO activated mTOR and decreased the protein level of ATG13 in the plaque endothelium of $apoE^{-/-}$ mice. Importantly, 3BDO did not affect the activity of mTOR and autophagy in macrophage cell line RAW246.7 and vascular smooth muscle cells of $apoE^{-/-}$ mice, but suppressed plaque endothelial cell death and restricted atherosclerosis development in the mice. 3BDO protected VECs by activating mTOR and thus stabilized atherosclerotic lesions in $apoE^{-/-}$ mice.

Atherosclerosis is a complex chronic inflammatory and metabolic disease. Atherosclerotic plaque destabilization and rupture leads to acute coronary syndromes that cause serious damage to human health worldwide[1]. However, we lack efficient therapy for atherosclerotic plaque stability. The endothelium, located at the interior surface of the vascular wall, acts as an effective permeable barrier between circulating blood and tissues. These cells also participate in the regulation of cell cholesterol, lipid homeostasis, signal transduction, immunity, inflammation and haemostasis[2]. Accumulating evidence suggests that endothelial cell (EC) injury may be detrimental to the structure of plaque, because endothelial death precedes atherogenesis and may also predispose to arterial thrombosis[3,4]. Protecting the endothelium against death has been considered a novel atherosclerotic treatment.

The protein kinase mammalian or mechanistic target of rapamycin (mTOR), also known as FK506 binding protein 12-rapamycin associated protein 1A, is an atypical serine/threonine kinase. mTOR is a critical regulator responding to upstream cellular signals, such as growth factors, energy, stress and nutrients, and participating in controlling cell growth and proliferation, protein synthesis, autophagy, ribosomal and mitochondrial biogenesis, and metabolism[5]. Dysregulation of mTOR signaling, particularly mTORC1, often occurs in human diseases including Alzheimer's disease, cancer and cardiovascular complications of diabetes[6]. Inhibiting mTOR with rapamycin confers protection against injury in the intact heart and adult cardiomyocytes, which is mediated by opening the mitochondrial ATP-sensitive potassium channel[7]. Furthermore, clinical data showed that implantation with the mTOR inhibitor drug-eluting stent (DES) has been successful in treating stable chronic angina or acute coronary syndrome[8]. Thus, mTOR inhibitors are currently being used in clinical trials[9]. mTOR may also be involved in the development of atherosclerotic plaque, and mTOR inhibitors inducing autophagy in

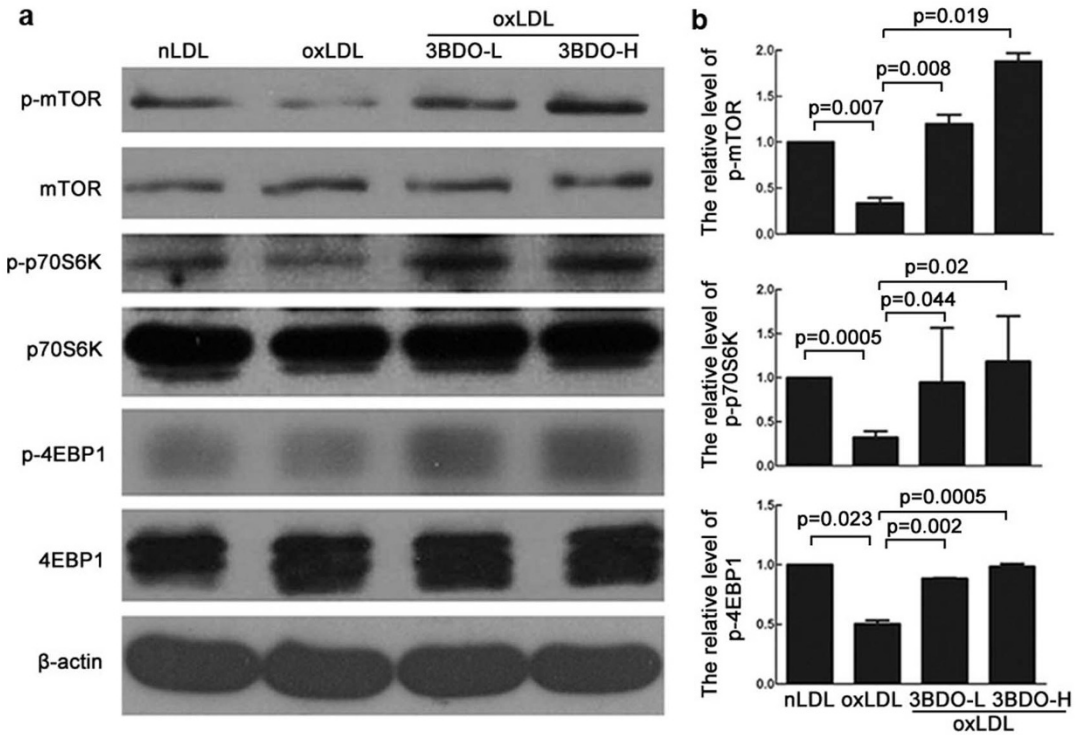

Figure 1 | Effect of 3BDO on mammalian target of rapamycin (mTOR) activity in oxidized low-density-lipoprotein (oxLDL)-treated human umbilical vein endothelial cells (HUVECs). (a), Western blot analysis of mTOR, phosphorylated mTOR (p-mTOR, Ser2448), p70S6K, phosphorylated p70S6K (p-p70S6K, Thr389), 4EBP1, phosphorylated 4EBP1(p-4EBP1, Thr37/46) in HUVECs treated with native LDL (nLDL), 50 μg/ml; oxLDL, 50 μg/ml; 3BDO-L, 60 μM; and 3BDO-H, 120 μM, for 12 h (cropped, full-length blots are in Supplementary Figure S6). (b), Densitometry results of ratio of p-mTOR to total mTOR, p-p70S6K to total p70S6K and p-4EBP1 to total 4EBP1. nLDL control data were set to 1. Data are mean ± SEM, n = 3.

macrophages were found to be potential plaque-stabilizing compounds[7,10,11]. However, drug-induced macrophage autophagy may lead to a pro-inflammatory response and postautophagic necrosis[12]. mTOR inhibitors were toxic in various cells, and inhibition of mTOR induced EC dysfunction and promoted arterial thrombosis *in vivo*, which may favor the development of thrombosis in DESs[13]. Moreover, mTOR inhibition led to EC death[14]. In addition, current *in vitro* and *in vivo* evidence suggests that the activation of mTOR is vital for endothelial growth. For example, in differentiated ECs, activation of mTOR inhibited both apoptosis and autophagy under oxidative stress via activating Akt[15]; inhibition of mTOR by various insults could lead to injured ECs and endothelial progenitor cells[14,16]. Recent study also revealed the protective role of mTOR signaling in angiogenesis and tissue regeneration[15]. Protecting the endothelium by activating mTOR might be a promising therapeutic strategy to prevent or treat atherosclerosis and other cardiovascular diseases.

We previously synthesized a series of butyrolactone derivatives and found that 3-benzyl-5-((2-nitrophenoxy) methyl)-dihydrofuran-2(3H)-one (3BDO, Supplemental Figure S1) could inhibit human umbilical vein EC (HUVEC) apoptosis and senescence induced by deprivation of serum and basic fibroblast growth factor 2[17]. Further study indicated that 3BDO selectively protected vascular ECs (VECs) and inhibited vascular smooth muscle cell (VSMC) proliferation and migration[18]. Moreover, 3BDO could inhibit the injury induced by chloroquine and lipopolysaccharide in HUVECs[19,20]. 3BDO may have a protective effect on VECs. In addition, we recently identified 3BDO as an activator of mTOR, which competitively binds to FK506-binding protein 1A, 12 kDa (FKBP1A)[21,22].

Here, we aimed to investigate whether 3BDO has a protective role via activating mTOR in ECs and thus stabilizing atherosclerotic lesions in apolipoprotein E-deficient (apoE$^{-/-}$) mice.

Results

3BDO inhibited oxLDL-decreased mTOR activity in HUVECs. We recently identified 3BDO as an activator of mTOR by targeting FKBP1A in HUVECs[22]. Here we further observed the effect of 3BDO on mTOR activity under oxLDL treatment in HUVECs. OxLDL inhibited the phosphorylation of mTOR and its downstream targets p70S6K and 4E-binding protein 1 (4EBP1), and 3BDO treatment reversed the oxLDL-inhibited phosphorylation of mTOR, p70S6K and 4EBP1 (Figure 1).

3BDO suppressed oxLDL-increased ATG13 protein level and altered the phosphorylation of ATG13 in HUVECs. ATG13 is a target of TOR signaling[23,24], and our recent work demonstrated that 3BDO could regulate ATG13 protein level[22]. Therefore, we detected total and phosphorylated ATG13 (p-ATG13, Ser318) in HUVECs treated with oxLDL or both 3BDO and oxLDL. OxLDL increased the total level of ATG13 and inhibited the level of p-ATG13 as compared with the nLDL control, and 3BDO inhibited the effect of oxLDL on ATG13 protein level (Figure 2a).

3BDO inhibited oxLDL-induced autophagy in HUVECs. Several previous studies from our lab revealed that 3BDO could modulate autophagy in HUVECs. Because ATG13 is necessary for autophagy initiation and 3BDO significantly inhibited oxLDL-increased ATG13 protein level and promoted its phosphorylation, we further observed whether 3BDO inhibited oxLDL-induced autophagy in HUVECs. The results of LC3-II level, p62 accumulation and LC3 puncta analysis showed that 3BDO inhibited oxLDL-induced autophagy (Figure 2b and c).

3BDO activated mTOR and decreased the level of ATG13 in the endothelium of apoE$^{-/-}$ mice. To further investigate the effect of

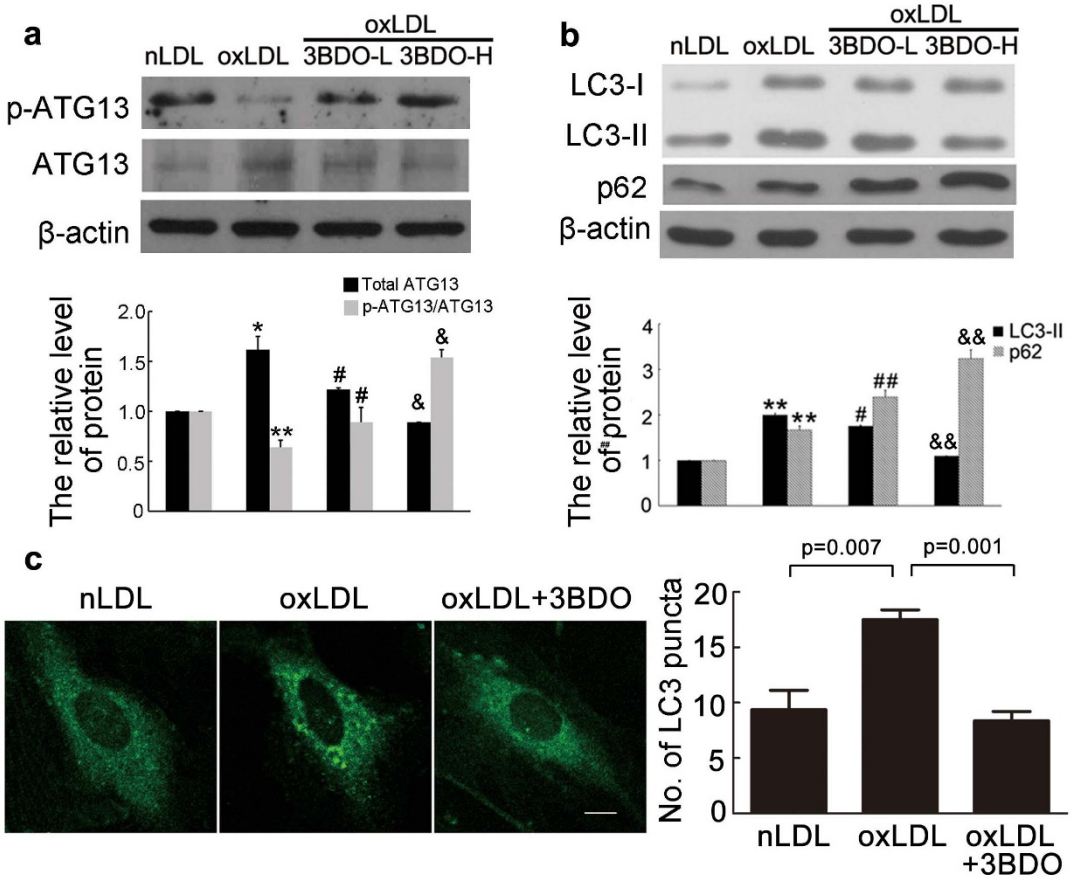

Figure 2 | Effect of 3BDO on oxLDL-induced autophagy in HUVECs. (a), Western blot analysis of ATG13 and p-ATG13 protein level and quantification (cropped, full-length blots are in Supplementary Figure S7), with nLDL, 50 μg/ml; oxLDL, 50 μg/ml; 3BDO-L, 60 μM; and 3BDO-H, 120 μM, for 12 h. nLDL control data were set to 1. Data are mean ± SEM; ATG13, *p=0.017 vs. nLDL, #p=0.024 vs. oxLDL, & p=0.024 vs. oxLDL; p-ATG13/ATG13, **p=0.004 vs. nLDL, #p=0.039 vs. oxLDL, & p=0.011vs. oxLDL. n=3. (b), Western blot analysis of LC3 –II and p62 and quantification (cropped, full-length blots are in Supplementary Figure S8), with nLDL, 50 μg/ml; oxLDL, 50 μg/ml; 3BDO-L, 60 μM; and 3BDO-H, 120 μM, for 12 h. Protein levels were normalized to that of β-actin. nLDL control data were set to 1. Data are mean ± SEM; LC3–II, **p=0.0008 vs. nLDL, #p=0.01 vs. oxLDL, &&p=0.0005 vs. oxLDL; p62, **p=0.004 vs. nLDL, ##p=0.003 vs. oxLDL, &&p=0.009 vs. oxLDL. n=3. (c), Immunofluorescence staining of LC3, with nLDL, 50 μg/ml; oxLDL, 50 μg/ml; 3BDO-L, 60 μM, for 12 h. Bar = 5 μM. Bar charts showed the quantification of average endogenous LC3 puncta per cell. Different fields of view (>3 regions) were analyzed on the microscope for each labeling condition, and representative results are shown. Data are mean ± SEM.

3BDO on the endothelium mTOR activity and autophagy *in vivo*, we assessed the level of p-p70S6K and ATG13 in plaque endothelium of apoE$^{-/-}$ mice. Immunofluorescence assay revealed that 3BDO treatment increased the level of p-p70S6K and decreased the protein level of ATG13 in plaque endothelium of apoE$^{-/-}$ mice, which confirmed that 3BDO activated endothelial mTOR and inhibited endothelial autophagy *in vivo* (Figures 3 and 4).

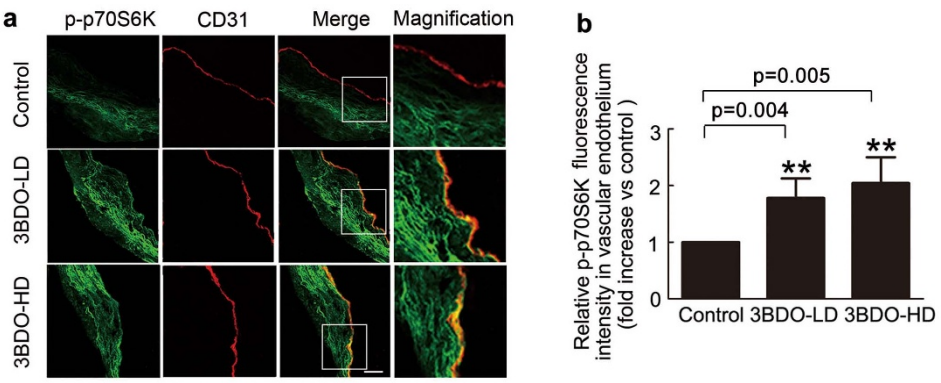

Figure 3 | 3BDO activated mTOR in the endothelium of apoE$^{-/-}$ mice. (a), Double-stained images of co-localization (yellow) of p-p70S6K with CD31-positive VECs of apoE$^{-/-}$ mice with and without 3BDO treatment. Bar = 60 μM. (b), Quantification of p-p70S6K protein level in a. Data are mean ± SEM. n = 6.

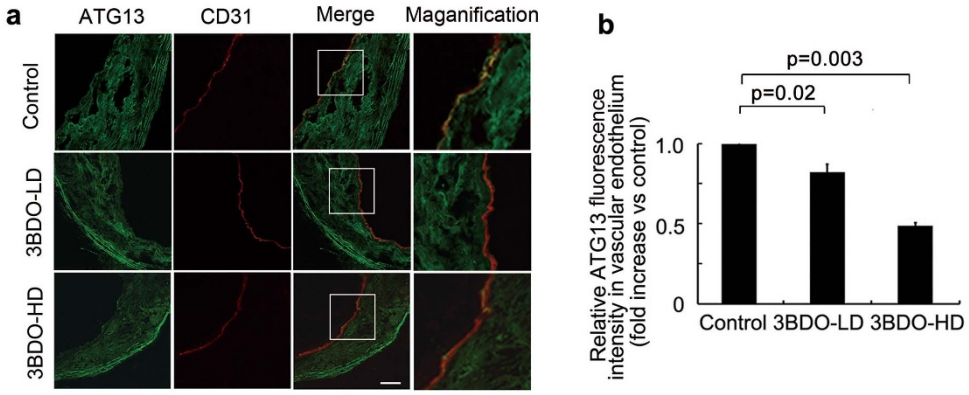

Figure 4 | 3BDO increased the level of ATG13 in the endothelium of apoE$^{-/-}$ mice. (a), Double-stained images of co-localization (yellow) of ATG13 with CD31-positive VECs of apoE$^{-/-}$ mice with and without 3BDO treatment. Bar = 60 μM. (b), Quantification of ATG13 protein level in a. Data are mean ± SEM. n =6.

3BDO did not affect oxLDL-activated mTOR and autophagy in macrophage cell line RAW246.7 and VSMCs of apoE$^{-/-}$ mice. To understand the cell specificity of 3BDO function, we further investigated the effect of 3BDO on oxLDL-activated mTOR and autophagy in macrophage cell line RAW246.7 and VSMCs of apoE$^{-/-}$ mice. 3BDO did not affect the phosphorylation of mTOR direct downstream targets p70S6K and 4EBP1 (Supplemental Figure S2). Meanwhile, 3BDO treatment did not change oxLDL-increased the level of LC3-II and ATG13 in RAW246.7 cells and VSMCs of apoE$^{-/-}$ mice (Supplemental Figure S3). Therefore, 3BDO selectively activated mTOR and inhibited oxLDL-triggered autophagy in VECs.

3BDO inhibited autophagy and apoptosis in the endothelium of apoE$^{-/-}$ mice. In atherosclerosis, excessively stimulated autophagy may cause VEC death. Therefore, we observed the effect of 3BDO on autophagy by *en face* staining of LC3 dots and apoptosis by TUNEL staining in plaque endothelium of apoE$^{-/-}$ mice. As compared with controls, apoE$^{-/-}$ mice showed inhibited endothelium autophagy and apoptosis with 3BDO treatment (Figure 5), so 3BDO protected against endothelium injury in atherosclerosis.

3BDO stabilized established atherosclerotic lesions and restricted atherosclerosis development in apoE$^{-/-}$ mice. To further elucidate the role of VEC mTOR in atherosclerosis, we examined the effect of 3BDO on atherosclerosis development in apoE$^{-/-}$ mice by detecting a series of indexes of atherosclerosis. Oil-red O staining of whole aortas (including aortic arch, thoracic and abdominal regions) and hematoxylin and eosin staining of aortic roots showed significantly decreased atherosclerotic lesion areas with 3BDO than control treatment (Figure 6a and b). 3BDO promoted the stability of plaque, with decreased the lipid deposition, increased the number of SMCs, reduced macrophage cell area and reduced matrix metalloproteinase 2 and 9 (MMP2/9) activity (Figure 6c). Therefore, 3BDO treatment stabilized established atherosclerotic lesions in apoE$^{-/-}$ mice.

3BDO inhibited the inflammatory response in apoE$^{-/-}$ mice and in oxLDL-treated HUVECs. Because atherosclerosis is a chronic inflammatory disease and hyperactivation of mTOR might be associated with inflammation, we further investigated the effect of 3BDO on the inflammatory response. 3BDO decreased oxLDL-induced upregulation of intracellular adhesion molecule 1 (ICAM-1) and vascular cell adhesion molecule 1 (VCAM-1), and inhibited oxLDL-induced secretion of IL-6 and IL-8 in HUVECs (Figure 7a–d). Moreover, in apoE$^{-/-}$ mice, as compared with controls, with 3BDO treatment, the serum level of IL-6 and IL-8 was significantly decreased (Figure 7e and f). Our data suggest that 3BDO inhibited atherosclerosis development and further alleviated the inflammatory response.

Discussion

Atherosclerotic plaque develops as a result of a chronic nonresolving inflammatory response involving dysfunction of the vascular endothelium. Therefore, the mechanism protecting the endothelium in atheromatous plaques is critical for the pathogenesis of atherosclerosis. mTOR is a highly conserved serine/threonine kinase and a central controller of cell growth, metabolism and aging and seems to be a potential therapeutic target for treating human diseases[25]. The mTOR inhibitors, rapamycin and its analogues, have been approved for prevention of restenosis following angioplasty and certain forms of cancer therapy[8,26]. The optimal mTOR inhibitor might be beneficial for patients with heart disease because mTOR activation is maladaptive during cardiac hypertrophy development and myocardial ischemia[27]. As well, mTOR has also been suggested to be involved in the development of atherosclerotic plaques and serves as a therapeutic target. Previous studies reported that inhibition of mTOR by sirolimus or everolimus decreased the number of macrophages by inducing autophagy and suppressng atherosclerosis[10,11]. Recent research also demonstrated that suppression of mTOR in an atherosclerotic mouse model by left ventricular-mediated RNAi inhibited atherosclerosis and stabilized plaques via a decrease of macrophages by autophagy[28]. Compared to macrophage activity, the elimination and injury of ECs is detrimental for atherosclerotic plaque stability. As well, mTOR is necessary for EC development because inhibition of mTOR pathways with various insults leads to EC injury[14–16]. For example, cigarette smoke components inhibited mTOR signaling in aortic endothelial cells, further upregulated matrix MMP-1 and caused angiogenesis injury[29]; mTOR inhibition is also involved in radiation-induced cardiovascular disease by contributing to premature senescence of HUVECs[30]. Moreover, mTOR inhibition during DES transplantation caused endothelial dysfunction and inflammation and promoted thrombus formation[31]. OxLDL, one of the culprits of atherosclerosis, could active mTOR during THP-1 macrophage foam cells formation and in rabbit femoral SMCs[32,33]. However, we found that oxLDL inhibited mTOR activity in VECs in this study. From our results and those of others, the effect of oxLDL on the mTOR pathway might be cell-type-specific. Meanwhile, 3BDO eliminated the oxLDL-induced inhibition of mTOR in VECs, but had no effect on mTOR in macrophage cell line RAW246.7. and VSMCs. Moreover, 3BDO significantly restrained atherosclerosis development in apoE$^{-/-}$ mice, so activating VEC mTOR might be a novel strategy for treatment of atherosclerosis.

Modulation of autophagy is one of the main mTOR-regulated processes and we have defined 3BDO as a small molecule regu-

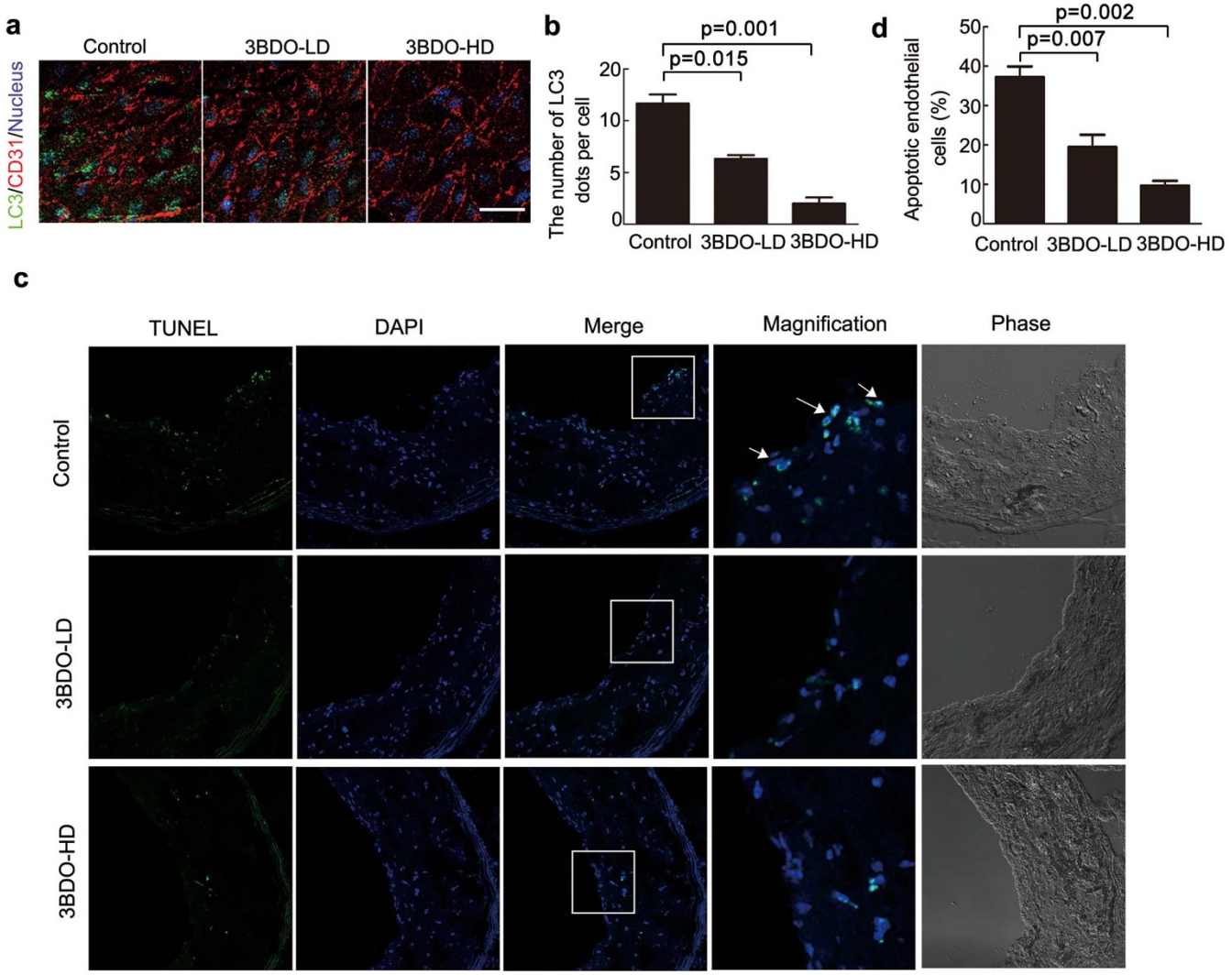

Figure 5 | 3BDO inhibited endothelium autophagy and apoptosis in apoE$^{-/-}$ mice. (a), *En face* staining of LC3 patches (green) in the thoracic aorta endothelium of apoE$^{-/-}$ mice. Endothelial cells were marked with CD31 (red). Nucleus (blue) was stained with DAPI. Bar = 60 μM. (b), Quantification of LC3 dots in the thoracic aorta endothelium. Data are mean ± SEM. n = 6. (c), Sections from the mice aortic roots were labeled by TUNEL to detect apoptotic cells and counterstained with DAPI to detect nuclei. The arrows indicated the TUNEL-positive cells. Bar = 60 μM. (d), Quantification of TUNEL-positive cells in the plaque endothelium. Data are mean ± SEM. n = 6.

lating autophagy in HUVECs[22]. Previous reports also demonstrated that oxLDL could induce VEC autophagy[32,34]. Autophagy is now known to become dysfunctional in atherosclerosis. Basal autophagy can protect plaque cells against oxidative stress by degrading damaged intracellular material[35]. However, excessively stimulated autophagy may cause VEC death, which in turn results in plaque destabilization as endothelial injury and/or death represents a primary mechanism for acute clinical events by promoting lesional thrombosis[36,37]. This evidence suggests that insufficient autophagy and hyperactivated autophagy of VECs are both detrimental and that regulating of autophagic homeostasis is crucial for treating atherosclerosis. Here, we found that 3BDO could inhibit oxLDL-induced autophagy in HUVECs and decrease the level of ATG13 and autophagy in the plaque endothelium of apoE$^{-/-}$ mice. However, the agent had no effect on the mTOR pathway or autophagy of macrophage RAW246.7 cells and VSMCs. Moreover, 3BDO inhibited the death of plaque endothelium in apoE$^{-/-}$ mice. 3BDO might selectively protect endothelial cells by modulating mTOR-dependent autophagy and thus restrict atherosclerosis development and stabilize established atherosclerotic lesions in apoE$^{-/-}$ mice.

The use of mTOR kinase inhibitors might damage tissues, and hyperactivation of mTOR might be associated with inflammation[6,26,38]. Here, we evaluated the effect of 3BDO on the weight of body and various organs in mice but found no significant difference in organ weights between controls and 3BDO-treated groups (Supplemental Table S1). We also found that 3BDO could inhibit inflammation response in oxLDL-treated HUVECs and apoE$^{-/-}$ mice. Therefore, 3BDO might be a potentially providing drug of therapeutic value.

In conclusion, as shown in Figure 8, we found that a butyrolactone derivative, 3BDO, via activating VEC mTOR, restricted atherosclerosis development and stabilized established atherosclerotic lesions in apoE$^{-/-}$ mice. Activation of mTOR might inhibit oxLDL-induced dephosphorylation of ATG13 and the increased ATG13 total protein level and thus suppress the death of plaque endothelium in apoE$^{-/-}$ mice.

Methods

Ethics statement. All experimental procedures and animal care were performed in accordance with the ARRIVE guidelines[39] and approved by the ethics committee in Shandong University.

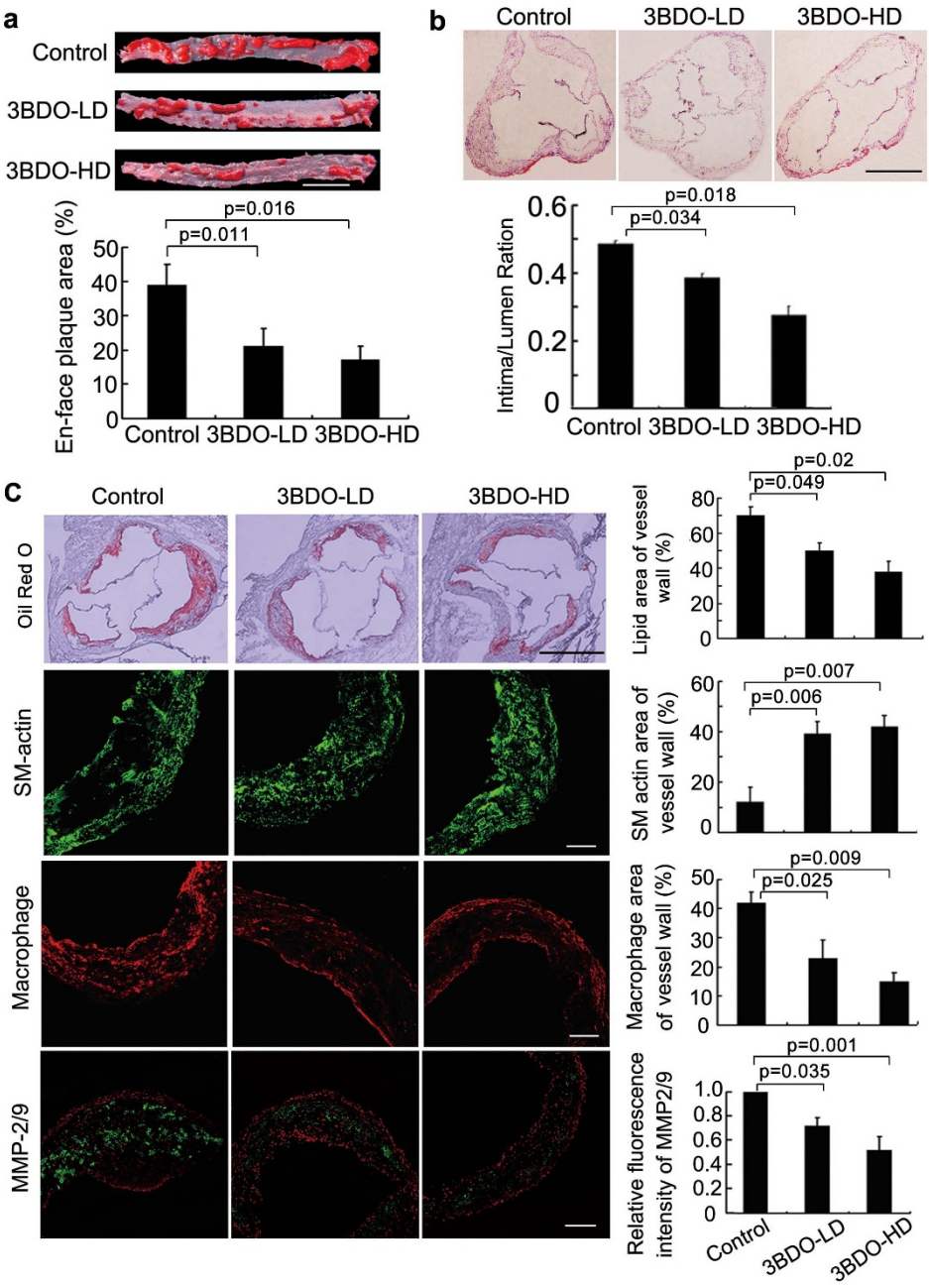

Figure 6 | Effect of 3BDO on the phenotype of aortic atherosclerotic plaque in apoE$^{-/-}$ mice. (a), Oil-red O staining of whole aortas and quantification. Data are mean ± SEM, Bar = 3 mm, n = 6. (b), Hematoxylin and eosin (H&E) staining and quantification of plaque area. Data are mean ± SEM. Bar = 500 μm. (c), From the top to bottom panel, Oil-red O staining of atherosclerotic lesions, immunofluorescence staining for mouse α-smooth muscle actin, Mac-3 (M3/84) and *in situ* zymography of matrix metalloproteinase 2/9 (MMP-2/9) activity. Bar for Oil-red O staining = 500 μm, others = 80 μm. D, Quantification of lipid area, smooth muscle area, macrophage area, and MMP-2/9 activity in control and 3BDO-treated groups. Data are mean ± SEM. n = 6.

Cell culture and treatment. HUVECs were extracted from human umbilical veins as described[40]. RAW246.7 cells were obtained from the Cell Bank of the Chinese Academy of Sciences (Shanghai, China). All cells were maintained at 37°C under humidified conditions and 5% CO_2. HUVECs were cultured on gelatin-coated plastic dishes in M199 medium (Gibco Laboratories, Grand Island, NY) with 20% (v/v) fetal bovine serum (Hyclone, SV30087.02) and 10 IU/mL fibroblast growth factor 2. All experiments involved HUVECs at no more than passage 10. RAW246.7 cells were cultured as routine in DMEM medium (Gibco Laboratories, Grand Island, NY) supplemented with 10% heat inactivated fetal bovine serum. Cells at 80% confluence were activated by oxLDL, 50 μg/ml; native LDL (nLDL), 50 μg/ml, was used as a control. For 3BDO treatment, cells were incubated with 60 or 120 μM 3BDO in the presence of oxLDL (50 μg/ml) for 12 h. nLDL and oxLDL treatment groups were supplemented with an equal amount of DMSO as a control.

Antibodies. Antibodies for p-p70S6K (9206), p70S6K (9202), and LC3 (2775) were from Cell Signaling Technology (Danvers, MA, USA); ATG13 (SAB4200100) was from Sigma (Sigma-Aldrich, St. Louis, MO); p62 (610833) was from BD Transduction Laboratories (San Jose, CA, USA); β-actin (sc-47778), α-actin (sc-130619), Mac-3 (M3/84) (sc-19991), CD31/PECAM-1 (sc-18916), ICAM-1(sc-7891), VCAM-1 (sc-8304) and horseradish peroxidase-conjugated secondary antibodies were all from Santa Cruz Biotechnology (Santa Cruz, CA, USA); Normal rabbit IgG (sc-2027) was a control for immunofluorescence assay. Secondary antibodies for immunofluorescence were goat anti-rabbit IgG Alexa Fluor-488 and goat anti-mouse IgG Alexa Fluor-633 (Invitrogen, Carlsbad, CA, USA).

Western blot analysis. Cell lysates were prepared in RIPA lysis buffer containing 25 mM Tris-HCl (pH 6.8), 2% SDS, 6% glycerol, 1% 2-mercaptoethanol, 2 mM PMSF, 0.2‰ bromphenol blue and a protease inhibitor cocktail. Vascular SMCs were

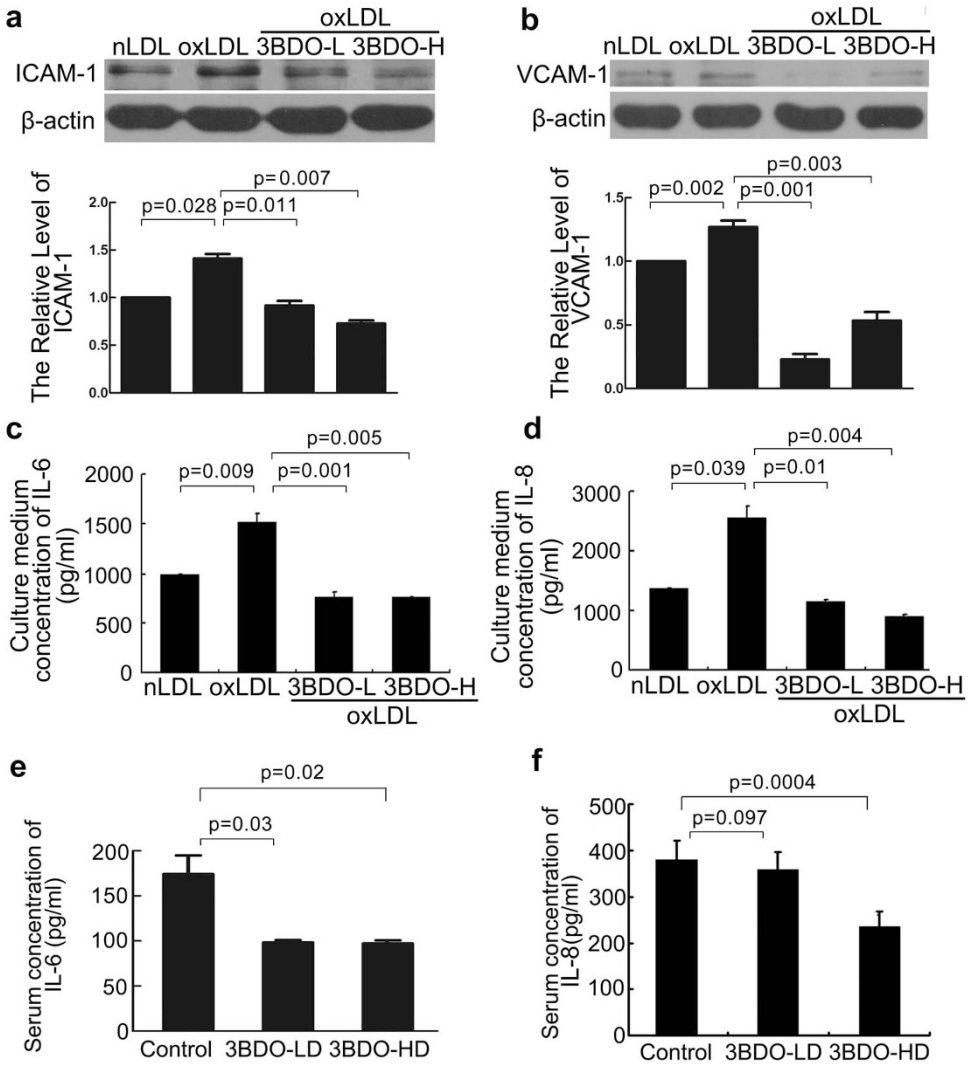

Figure 7 | Effect of 3BDO on inflammatory response in oxLDL-treated HUVECs and apoE$^{-/-}$ mice. (a) and (b), Western blot analysis of the effect of 3BDO on intracellular adhesion molecule 1 (ICAM-1) and vascular cell adhesion molecule 1 (VCAM-1) level (full-length blots are in Supplementary Figure S9 and S10), with oxLDL, 50 μg/ml; 3BDO-L, 60 μM; 3BDO-H, 120 μM for 12 h. Protein levels were normalized to that of β-actin. Data are mean ± SEM. n = 3. (c) and (d), ELISA of the secretion of interleukin 6 (IL-6) and IL-8 from HUVECs with 3BDO treatment. oxLDL, 50 μg/ml; 3BDO-L, 60 μM; 3BDO-H, 120 μM for 12 h. Data are mean ± SEM. n = 3. (e) and (f), ELISA of the secretion of interleukin 6 (IL-6) and IL-8 in serum of apoE$^{-/-}$ mice. Data are mean ± SEM. n = 6.

extracted as follows: mouse aortas were opened longitudinally and scraped off the endothelium and vascular adventitia,then lysed with RIPA lysis buffer. Protein samples were loaded and separated on a 15% SDS-polyacrylamide gel and electrophoretically transferred to a polyvinylidenedifluoride (PVDF) membrane (Millipore, Schwalbach, Germany), which was incubated with primary antibodies (1 : 1000), then horseradish peroxidase-linked secondary antibodies (1 : 5000). Bands were detected by use of an enhanced chemiluminesence detection kit (Thermo Electron Corp., Rockford, USA). The relative quantity of proteins was analyzed by use of Quantity one software and normalized to that of loading controls.

Cell staining for immunofluorescence microscopy. Treated HUVECs were fixed with 4% paraformaldehyde for 15 min and blocked with 3% normal goat serum or rabbit serum for 20 min at room temperature, and incubated with anti-LC3 antibody (1 : 100) overnight at 4°C. Then cells were rinsed in 0.1 mol/L phosphate buffered saline 3 times and incubated with corresponding secondary antibody (1 : 200) 1 h at 37°C and evaluated by laser-scanning confocal microscopy. For negative controls, cells were incubated with normal IgG.

Animal model. Male apoE$^{-/-}$ mice (8 weeks old; C57BL/6J-knockout) were purchased from the Department of Laboratory Animal Science, Peking University Health Science Center, China, and used to build the atherosclerosis animal model. All *in vivo* experiments followed the ARRIVE guidelines[39]. The experimental method is shown in online-only Data Supplement Figure S4. ApoE$^{-/-}$ mice were fed an atherogenic diet (containing 21% fat and 0.15% cholesterol). To avoid the potential confounding effects of variation among batches of diet, a single batch was reserved and used throughout the experiment. Mice at 20 weeks older were divided into 3 groups of for treatment (n=8 mice/group) for 8 weeks: control (DMSO), low-dose 3BDO (50 mg/kg/d; 3BDO-L) and high-dose 3BDO (100 mg/kg/d; 3BDO-H).

Blood and tissue collection and organ coefficients. The body weight of mice was measured every week during 3BDO injection. Blood samples were taken from the inferior vena cava, and animals were killed by exsanguination. Blood was centrifuged to obtain serum. The heart and whole aorta were immediately extracted. The aortic roots were embedded in optimal cutting temperature (OCT) embedding medium (Tissue-Tek, Sakura Finetek USA, Torrance, CA) for histology and immunofluorescence assay. The remaining aorta was longitudinally opened and fixed with 4% paraformaldehyde for lipid measurement at the surface of the vascular wall. The embedded aortas were kept at −80°C. The other organs, including heart, liver, spleen, lungs, kidney, and brain, were extracted and weighed. The organ coefficient was obtained by dividing the weight of the organ by body weight.

Histology and immunofluorescence. The aortic roots were embedded in OCT embedding medium. Cryosections of aortic sinus (7 μm) were prepared and stained with hematoxylin and eosin (Sigma-Aldrich, Zwijndrecht, The Netherlands). Aortic sinus cryosections, 10 μm, underwent Oil-red O (Sigma-Aldrich, Zwijndrecht, The Netherlands) staining. Images of sections were analyzed by use of ImagePro Plus. Corresponding sections (7 μm) were stained with primary antibodies (1 : 200) overnight at 4°C. After incubation with the appropriate secondary antibodies (1 : 500) at 37°C for 1 h, sections were observed by confocal laser scanning microscopy (Zeiss LSM780, Carl Zeiss Canada). The negative control was nonimmune IgGs

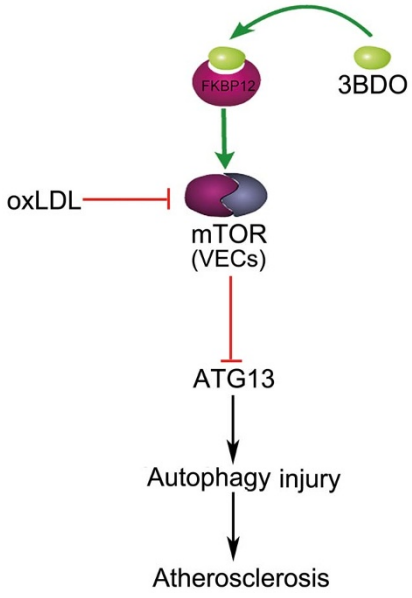

Figure 8 | Conceptual schematic of 3BDO and mTOR action mechanism in atherosclerosis. OxLDL could induce mTOR inhibition, and the inhibition of mTOR contributes to autophagy by increasing the protein level of ATG13 and inhibiting ATG13 phosphorylation. The excessively stimulated autophagy finally leads to endothelial injury of apoE-/- mice. 3BDO could reverse oxLDL-induced mTOR inhibition in VECs and inhibit oxLDL-induced ATG13 increase and dephosphorylation, thus relieving oxLDL-induced autophagy injury and inhibiting atherosclerosis development in apoE$^{-/-}$ mice.

(Supplementary Figure S5). Eight sections per mouse were analyzed and sections were selected every 70 μm.

En Face staining of plaque area. En face staining of plaque area in mice was measured as described. Briefly, after tissues were trimmed from around the aorta, the aorta (including aortic arch, thoracic and abdominal regions) was opened longitudinally, pinned on a cork board, and stained with Oil-red O (Sigma-Aldrich, Zwijndrecht, The Netherlands) to detect lipids and to determine lesion area. En face images of the aorta were taken with a digital camera (Canon EOS 7D, Canon Corp., Tokyo, Japan) and analyzed by use of ImagePro Plus. Atherosclerotic lesions of the aorta were expressed as a percentage of the total surface area.

***En face* immunofluorescence staining.** For *en face* staining of LC3 patches in aorta endothelium, thoracic aortas were opened longitudinally and cut into 0.09-cm^2 square pieces. The aorta segments were fixed in 4% paraformaldehyde for 10 min at room temperature, then vascular tissues were permeabilized with 0.2% Triton X-100 for 10 min at room temperature. To eliminate non-specific binding, aorta segments were incubated with 10% horse serum for 30 min at room temperature, antibodies for LC3 and CD31 at 4°C overnight, then secondary antibodies for 1 h at 37°C. The nuclei were stained with DAPI. Aorta segments were pinned flat with the endothelium facing up on glass slides, and LC3 patches were evaluated by confocal laser scanning microscopy.

Apoptotic cells in atherosclerotic lesions of apoE$^{-/-}$ mice. Apoptotic cells in atherosclerotic plaque were detected by terminal deoxynucleotidyl transferase (TdT)-mediated dUTP nick end labeling (TUNEL) with use of a kit (R&D Systems). After TUNEL labeling, sections were counterstained with DAPI to detect nuclei.

***In situ* zymography.** Mouse aortic sections were incubated with 50 ml of 10 mg/ml quenched FITC-labeled DQ gelatin (Invitrogen) and 1 mg/ml propidium iodide (PI, Sigma-Aldrich, St. Louis, MO) in 0.5% low-melting-point agarose (Invitrogen), cover-slipped, and chilled for 5 min at 4°C. Sections were incubated at 37°C for 2 h and observed by fluorescence microscopy. Gelatinase inhibitor (matrix metalloproteinase 2 [MMP-2]/9 inhibitor IV, Chemicon, Millipore) was added as a control. Carl Zeiss AxioVision 4.6 was used to measure the fluorescence intensity in at least 8 sections from each aortic root sample.

Enzyme-linked immunosorbent assay (ELISA). The level of IL-6 or IL-8 in serum from apoE$^{-/-}$ mice and in culture medium was determined by use of mouse and human ELISA kits (R&D Systems, Minneapolis, MN). The data were analyzed by applying the provided standard.

Statistical analysis. Data are presented as mean ± SEM. Statistical analyses involved SPSS 11.5 (SPSS Inc., Chicago, IL). Images were processed by use of Graphpad Prism 5 (GraphPad Software, La Jolla, CA, USA) and Adobe Photoshop (Adobe, San Jose, USA). At least 3 independent replications were performed. Data were compared by one-way ANOVA. $p<0.05$ was considered statistically significant.

1. Rioufol, G. *et al.* Multiple atherosclerotic plaque rupture in acute coronary syndrome: a three-vessel intravascular ultrasound study. *Circulation* **106**, 804–808 (2002).
2. Simionescu, M. & Antohe, F. Functional ultrastructure of the vascular endothelium: changes in various pathologies. *Handb. Exp. Pharmacol.* **176 Pt 1**, 41–69 (2006).
3. Sima, A. V., Stancu, C. S. & Simionescu, M. Vascular endothelium in atherosclerosis. *Cell. Tissue. Res.* **335**, 191–203 (2009).
4. Rajendran, P. *et al.* The Vascular Endothelium and Human Diseases. *Int. J. Biol. Sci.* **9**, 1057–1069 (2013).
5. Weichhart, T. Mammalian target of rapamycin: a signaling kinase for every aspect of cellular life. *Methods. Mol. Biol.* **821**, 1–14 (2012).
6. Laplante, M. & Sabatini, D. M. mTOR signaling in growth control and disease. *Cell* **149**, 274–293 (2012).
7. Khan, S. *et al.* Rapamycin confers preconditioning-like protection against ischemia-reperfusion injury in isolated mouse heart and cardiomyocytes. *J. Mol. Cell. Cardiol.* **41**, 256–264 (2006).
8. Niccoli, G. *et al.* Impact of gender on clinical outcomes after mTOR-inhibitor drug-eluting stent implantation in patients with first manifestation of ischaemic heart disease. *Eur. J. Prev. Cardiol.* **19**, 914–926 (2012).
9. Santulli, G. & Totary-Jain, H. Tailoring mTOR-based therapy: molecular evidence and clinical challenges. *Pharmacogenomics* **14**, 1517–1526 (2013).
10. Elloso, M. M. *et al.* Protective effect of the immunosuppressant sirolimus against aortic atherosclerosis in apo E-deficient mice. *Am. J. Transplant.* **3**, 562–569 (2003).
11. Verheye, S. *et al.* Selective clearance of macrophages in atherosclerotic plaques by autophagy. *J. Am. Coll. Cardiol.* **49**, 706–715 (2007).
12. Martinet, W. *et al.* Drug-induced macrophage autophagy in atherosclerosis: for better or worse? *Basic. Res. Cardiol.* **108**, 321 (2013).
13. Camici, G. G. *et al.* Rapamycin promotes arterial thrombosis in vivo: implications for everolimus and zotarolimus eluting stents. *Eur. Heart. J.* **31**, 236–242 (2010).
14. Miriuka, S. G. *et al.* mTOR inhibition induces endothelial progenitor cell death. *Am. J. Transplant.* **6**, 2069–2079 (2006).
15. Chong, Z. Z., Shang, Y. C. & Maiese, K. Cardiovascular disease and mTOR signaling. *Trends. Cardiovasc. Med.* **21**, 151–155 (2011).
16. Humar, R., Kiefer, F. N., Berns, H., Resink, T. J. & Battegay, E. J. Hypoxia enhances vascular cell proliferation and angiogenesis in vitro via rapamycin (mTOR)-dependent signaling. *FASEB. J.* **16**, 771–780 (2002).
17. Wang, W. *et al.* Both senescence and apoptosis induced by deprivation of growth factors were inhibited by a novel butyrolactone derivative through depressing integrin beta4 in vascular endothelial cells. *Endothelium* **14**, 325–332 (2007).
18. Meng, N. *et al.* A novel butyrolactone derivative inhibited smooth muscle cell migration and proliferation and maintained endothelial cell functions through selectively affecting Na, K-ATPase activity and mitochondria membrane potential during in vitro angiogenesis. *J. Cell. Biochem.* **104**, 2123–2130 (2008).
19. Huang, B. *et al.* Protective effects of a synthesized butyrolactone derivative against chloroquine-induced autophagic vesicle accumulation and the disturbance of mitochondrial membrane potential and Na+,K+-ATPase activity in vascular endothelial cells. *Chem. Res. Toxicol.* **22**, 471–475 (2009).
20. Meng, N. *et al.* A butyrolactone derivative suppressed lipopolysaccharide-induced autophagic injury through inhibiting the autoregulatory loop of p8 and p53 in vascular endothelial cells. *Int. J. Biochem. Cell. Bio.* **44**, 311–319 (2012).
21. Yang, S. *et al.* Butyrolactone derivative 3-benzyl-5-((2-nitrophenoxy) methyl)-dihydrofuran-2(3H)-one protects against amyloid-beta peptides-induced cytotoxicity in PC12 cells. *J. Alzheimers. Dis.* **28**, 345–356 (2012).
22. Ge, D. *et al.* Identification of a novel mTOR activator and discovery of a competing endogenous RNA regulating autophagy in vascular endothelial cells. *Autophagy* **10**, 957–971 (2014).
23. Mercer, C. A., Kaliappan, A. & Dennis, P. B. A novel, human Atg13 binding protein, Atg101, interacts with ULK1 and is essential for macroautophagy. *Autophagy* **5**, 649–662 (2009).
24. Hosokawa, N. *et al.* Nutrient-dependent mTORC1 association with the ULK1-Atg13-FIP200 complex required for autophagy. *Mol. Biol. Cell.* **20**, 1981–1991 (2009).
25. Johnson, S. C., Rabinovitch, P. S. & Kaeberlein, M. mTOR is a key modulator of ageing and age-related disease. *Nature* **493**, 338–345 (2013).
26. Easton, J. B. & Houghton, P. J. Therapeutic potential of target of rapamycin inhibitors. *Expert. Opin. Ther. Targets.* **8**, 551–564 (2004).
27. Sciarretta, S., Volpe, M. & Sadoshima, J. Mammalian target of rapamycin signaling in cardiac physiology and disease. *Circ. Res.* **114**, 549–564 (2014).
28. Wang, X. *et al.* Knockdown of mTOR by lentivirusmediated RNA interference suppresses atherosclerosis and stabilizes plaques via a decrease of macrophages by autophagy in apolipoprotein Edeficient mice. *Int. J. Mol. Med.* **32**, 1215–1221 (2013).

29. Lemaitre, V., Dabo, A. J. & D'Armiento, J. Cigarette smoke components induce matrix metalloproteinase-1 in aortic endothelial cells through inhibition of mTOR signaling. *Toxicol. Sci.* **123**, 542–549 (2011).
30. Yentrapalli, R. *et al*. The PI3K/Akt/mTOR pathway is implicated in the premature senescence of primary human endothelial cells exposed to chronic radiation. *PloS one* **8**, e70024 (2013).
31. Pendyala, L. K. *et al*. The first-generation drug-eluting stents and coronary endothelial dysfunction. *JACC. Cardiovasc. Interv.* **2**, 1169–1177 (2009).
32. Zabirnyk, O., Liu, W., Khalil, S., Sharma, A. & Phang, J. M. Oxidized low-density lipoproteins upregulate proline oxidase to initiate ROS-dependent autophagy. *Carcinogenesis* **31**, 446–454 (2010).
33. Yu, M., Kang, X., Xue, H. & Yin, H. Toll-like receptor 4 is up-regulated by mTOR activation during THP-1 macrophage foam cells formation. *Acta. Biochim. Biophys. Sin.* **43**, 940–947 (2011).
34. Ding, Z. *et al*. Oxidant stress in mitochondrial DNA damage, autophagy and inflammation in atherosclerosis. *Sci. Rep.* **3**, 1077 (2013).
35. Martinet, W. & De Meyer, G. R. Autophagy in atherosclerosis: a cell survival and death phenomenon with therapeutic potential. *Circ. Res.* **104**, 304–317 (2009).
36. Levine, B. & Yuan, J. Autophagy in cell death: an innocent convict? *J. Clin. Invest.* **115**, 2679–2688 (2005).
37. Schrijvers, D. M., De Meyer, G. R. & Martinet, W. Autophagy in atherosclerosis: a potential drug target for plaque stabilization. *Arterioscler. Thromb. Vasc. Biol.* **31**, 2787–2791 (2011).
38. Barlow, A. D., Nicholson, M. L. & Herbert, T. P. Evidence for rapamycin toxicity in pancreatic beta-cells and a review of the underlying molecular mechanisms. *Diabetes* **62**, 2674–2682 (2013).
39. Kilkenny, C., Browne, W. J., Cuthill, I. C., Emerson, M. & Altman, D. G. Improving bioscience research reporting: the ARRIVE guidelines for reporting animal research. *PLoS. Biol.* **8**, e1000412 (2010).
40. Jaffe, E. A., Nachman, R. L., Becker, C. G. & Minick, C. R. Culture of human endothelial cells derived from umbilical veins. Identification by morphologic and immunologic criteria. *J. Clin. Invest.* **52**, 2745–2756 (1973).

Acknowlegments

This study was funded in part by the National 973 Research Project (No. 2011CB503906), National Natural Science Foundation of China (Nos. 91313303, 81321061, 31270877, 31070735, 31200859, 20972088 and J1103515), China Postdoctoral Science Foundation (No. 2014M551895), Shandong Excellent Young Scientist Award Fund (BS2013SW010).

Author contributions

J.Y.M., B.X.Z. and Y.Z. designed the experiments. N.P. and N.M. performed the experiments, analysed the data and prepared the figures. S.Q.W. synthesized the small molecular 3BDO. J.Z., L.S., F.Z. and S.L.Z. participated in animal model design. N.P. and N.M. wrote the main text. All authors reviewed the manuscript.

Additional information

Supplementary information accompanies this paper at http://www.nature.com/scientificreports

Competing financial interests: The authors declare no competing financial interests.

How to cite this article: Peng, N. *et al.* An activator of mTOR inhibits oxLDL-induced autophagy and apoptosis in vascular endothelial cells and restricts atherosclerosis in apolipoprotein $E^{-/-}$ mice. *Sci. Rep.* **4**, 5519; DOI:10.1038/srep05519 (2014).

This work is licensed under a Creative Commons Attribution-NonCommercial-NoDerivs 4.0 International License. The images or other third party material in this article are included in the article's Creative Commons license, unless indicated otherwise in the credit line; if the material is not included under the Creative Commons license, users will need to obtain permission from the license holder in order to reproduce the material. To view a copy of this license, visit http://creativecommons.org/licenses/by-nc-nd/4.0/